

A single-day mouse mesenteric lymph surgery in mice: an updated approach to study dietary lipid absorption, chylomicron secretion, and lymphocyte dynamics

Nikolaos Dedousis, Lihong Teng, Jitendra S. Kanshana, and Alison B. Kohan*

Department of Medicine, Division of Endocrinology and Metabolism, University of Pittsburgh, School of Medicine, Pittsburgh, PA, USA

Abstract The intestine plays a crucial role in regulating whole-body lipid metabolism through its unique function of absorbing dietary fat. In the small intestine, absorptive epithelial cells emulsify hydrophobic dietary triglycerides (TAGs) prior to secreting them into mesenteric lymphatic vessels as chylomicrons. Except for short- and medium-chain fatty acids, which are directly absorbed from the intestinal lumen into portal vasculature, the only way for an animal to absorb dietary TAG is through the chylomicron/mesenteric lymphatic pathway. Isolating intestinal lipoproteins, including chylomicrons, is extremely difficult *in vivo* because of the dilution of postprandial lymph in the peripheral blood. In addition, once postprandial lymph enters the circulation, chylomicron TAGs are rapidly hydrolyzed. To enhance isolation of large quantities of pure postprandial chylomicrons, we have modified the Tso group's highly reproducible gold-standard double-cannulation technique in rats to enable single-day surgery and lymph collection in mice. Our technique has a significantly higher survival rate than the traditional 2-day surgical model and allows for the collection of greater than 400 μ l of chylous lymph with high postprandial TAG concentrations. Using this approach, we show that after an intraduodenal lipid bolus, the mesenteric lymph contains naïve CD4⁺ T-cell populations that can be quantified by flow cytometry.  In conclusion, this experimental approach represents a quantitative tool for determining dietary lipid absorption, intestinal lipoprotein dynamics, and mesenteric immunity. Our model may also be a powerful tool for studies of antigens, the microbiome, pharmacokinetics, and dietary compound absorption.

Supplementary key words small intestine • mesenteric lymph • lipoproteins • metabolism • dietary fat • enterocytes • fatty acid/transport • lymphocytes • triglycerides • CD4⁺ T cells • postprandial lipids

The intestine plays a crucial physiological role in whole-body lipid metabolism through dietary fat absorption. In the small intestine, absorptive epithelial

cells emulsify hydrophobic dietary triglycerides (TAGs) prior to secreting them into the mesenteric lymphatics as chylomicron particles (1). Dietary TAG first enters the duodenum and is hydrolyzed by pancreatic lipase in the small intestinal lumen. Free fatty acids and monoacylglycerol, which are hydrolysis products of dietary TAG, are then absorbed into the enterocyte, resynthesized into TAG, and packaged into chylomicrons (reviewed here (2, 3)). Mature chylomicrons are then secreted through the basolateral membrane into the mesenteric lymphatics (4). Except for short- and medium-chain TAG, which are directly absorbed from the intestinal lumen into portal blood, the only way for an animal to absorb dietary TAG is through this chylomicron/mesenteric lymphatic pathway (5, 6).

The human small intestine is almost always secreting lipoproteins. These include intestinal HDLs, a major pathway for cholesterol absorption; intestinal VLDL that can contribute up to ~11% of the TAG in plasma; and the major intestinal lipoprotein, the chylomicron, which is the major carrier of dietary TAG (7–9). Chylomicrons are secreted as early as 13 min after a lipid meal and reach their peak secretion rate at ~2 h after a meal (10). Chylomicron secretion continues over the next ~6 h, which is considered the postprandial period (11). Several studies have demonstrated that oral glucose can also mobilize stored intracellular TAG in enterocytes and can potentiate the secretion of lipid-poor chylomicrons for up to 16 h after the last meal (12, 13).

While chylomicron assembly is largely driven by TAG in the diet, there are situations where enterocyte *de novo* lipogenesis can also provide fatty acids for intestinal lipoproteins (14). An important example is during the fasting state, when apical fatty acids are absent, yet the small intestine still secretes apoB48-containing particles (essentially a constitutive intestinal VLDL) (8, 15, 16). In addition, there is evidence that diet-induced insulin resistance and hypertriglyceridemia results in the overproduction of both chylomicrons and intestinal VLDL, and that these

*For correspondence: Alison B. Kohan, akohan@pitt.edu.

particles are loaded with TAG that comes from de novo synthesized and plasma fatty acids (17–19). Therefore, by the time most people are ready to eat their next meal, they are still in the postprandial state of the previous meal, and even when they enter a fasting period, the small intestine still secretes apoB-containing particles with TAG and cholesterol.

Diseases where dietary fat absorption is defective include inflammatory bowel disease, cystic fibrosis, short bowel syndrome, intestinal wasting diseases (20, 21), and lysosomal acid lipase deficiencies (like Wolman disease or cholesterol ester storage disease) (22–25). Defective dietary fat absorption is not simply an inability to extract fat from a meal (since the gut can adapt to defects in surface area and length), it also results in the use of noncanonical absorption pathways that form abnormal and potentially dysfunctional chylomicrons. There are many molecular events that have dramatic effects on chylomicron secretion; these include intracellular dysfunction in dietary TAG absorption and intracellular resynthesis (26–29), endoplasmic reticulum events like the lipidation of nascent chylomicrons (30, 31), and changes in the source of chylomicron TAG (i.e., from dietary fatty acids, or less frequently, from de novo fatty acids and glycerol phosphate) (32, 33). The net result is often a rescue of total fat absorption but at the cost of normal chylomicron synthesis and secretion.

A key component of chylomicrons are their apolipoproteins, which regulate multiple metabolic events. ApoB-48 is the structural protein making up chylomicrons (30, 34–36). ApoC-III and apoC-II work in opposition to each other to tightly regulate the clearance of chylomicron TAG from blood into tissues (apoC-III inhibits LPL hydrolysis (37) and LDL receptor-mediated endocytosis (38), respectively, and apoC-II stimulates LPL activity (39)). Chylomicrons acquire apoE in the plasma, which is required for the ultimate clearance of remnant chylomicrons from blood into the liver (40). Together, these activities of apolipoproteins are crucial to ensuring not only that extraintestinal tissues have access to dietary TAG but also that TAG is also efficiently removed from the circulation into the liver.

When apolipoproteins are missing or defective, dietary TAG is not metabolized normally. For example, chylomicrons containing excess apoC-III inhibit LPL and LDL receptor clearance pathways so successfully that these particles are retained in plasma and cause severe hyperlipidemia (41–44). Interestingly, excess apoC-II is also associated with reduced LPL activity and hypertriglyceridemia (45, 46). Clinically, dysfunction in the clearance of chylomicron TAG from blood is a major clinical problem (47–49). Children with short bowel disease, or patients missing small intestine, are often treated with parental intravenous lipids, which contain emulsified TAG but not apolipoproteins (48, 50). Though this effectively delivers soluble TAG to the blood (like chylomicrons do), the bulk of intravenous

lipids is rapidly cleared by the liver, resulting in fatty liver and inefficient calorie replenishment (50, 51). This clinical scenario highlights the physiological importance of chylomicrons and the critical role of the intestine in the postprandial state.

Causes of abnormal chylomicron synthesis include: 1) inability to maintain the primary site of lipid absorption: The proximal duodenum and jejunum have the highest fat absorption and chylomicron synthesis capacity (52). If dietary fat is unabsorbed in these proximal locations, and instead travels to the ileum, the chylomicrons produced will often contain less TAG but more bacterial lipopolysaccharide (LPS) per particle (53, 54). Bacterial LPS is known to travel through enterocytes, and during this process, it can be incorporated on chylomicrons. The amount of LPS can be temporarily reduced when chylomicron secretion is blocked with Pluronic L81 (55), but the dynamics of this process are not clear. 2) Defects in the trafficking of dietary TAG through absorptive enterocytes: there are three regulated steps of dietary lipid absorption—luminal hydrolysis and fatty acid traffic through the unstirred water layer into the mucosa, intracellular fatty acid re-esterification into TAG, and enterocyte chylomicron secretion into lymph. Dysfunction at each step yields small dense chylomicrons or chylomicrons containing inappropriate apoproteins. These changes can lead to either inefficient metabolism of chylomicrons by lipases on peripheral tissues and chylomicron retention in the blood (56, 57), or alternatively, can cause chylomicrons to speed through the vasculature avoiding tissue lipid delivery and instead load the liver with dietary fat (as in chylomicrons lacking apoC-III or containing excess apoC-II) (58–60). This deprives peripheral tissues of metabolic substrates (61). These processes are an underappreciated mechanism in how the small intestine can direct whole-body metabolism.

Because of these complexities in chylomicron character, metabolism, and formation, it is difficult to find a direct replacement or comparator for mechanistic studies (62, 63). Our group and many others routinely use fatty acids bound to albumin or lipid emulsions because they are so much simpler to prepare and dose than chylomicrons (64–68). Isolating intestinal lipoproteins is not trivial. Chylomicron remnants can be isolated from plasma via ultracentrifugation in the 2–6 h after a gavage, but these particles will be a mixture of partially hydrolyzed chylomicrons varying in size and TAG content (69). It is also difficult to isolate a large quantity of chylomicron remnants from plasma, especially in quantities needed for cell culture experiments. Another approach is to cannulate the thoracic lymph duct prior to its intersection with the subclavian vein, which will capture mesenteric lymph as it enters the circulation (70). Again, large quantities of lymph are difficult to obtain using this approach. Finally, lymph can be statically sampled from the mesenteric lymph duct at a single time point after a lipid meal (71, 72).

This approach requires perfusion of the gut but does not allow for terminal measurement of the movement of dietary lipids through the gastrointestinal tract or their absorption capacity between the lumen and enterocytes. Lymph volumes are also quite small.

It should also be emphasized that intestinal lymphatic system is not merely a passive duct for drainage of fats and for fluid balance. Lymph is an immune compartment. In addition to absorbing dietary TAG and other nutrients, the intestine must also regulate immune homeostasis in response to intestinal microbiota while maintaining vigilance against infectious microorganisms. This task is complex; microbiota contain a multitude of antigens, expressed on organisms that have heterogeneous interactions with the host and are constantly changing both in composition and behavior. In addition, the immune response must also remain sensitive to inflammatory signals produced by damaged or infected enterocytes. There is a major interest in the dynamics of inflammatory versus suppressive lymphocytes in the small intestine, and the mesenteric lymph (both postnodal and prenodal compartments) is a major site of these dynamics (72–74).

Using the Tso Lab's highly reproducible gold-standard double-cannulation technique as the foundation for our studies, we now describe a 1-day surgical model for isolating mesenteric lymph. Our procedure differs from previous design by reducing the surgery and experimental period to a single day, improving TAG excursion in response to duodenal lipids, and dramatically improving surgical success rate, which reduces the number of experimental animals needed.

MATERIALS AND METHODS

Animals

C57BL/6J mice were obtained from Jackson Labs (Bar Harbor, ME), and in-house bred WT mice aged 8–14 weeks were used. All mice were housed on a 12-h light/dark cycle with ad libitum access to standard chow and water. Whether mice are fasted overnight or not will depend on the experimental design. In practice, we find that an overnight fast is not necessary unless we are concerned about differences in rate of stomach emptying. For all experiments presented here, mice were not fasted overnight prior to surgery. All surgical procedures were approved by the University of Pittsburgh Internal Animal Care and Use Committee (protocol #20047008) and comply with the National Institutes of Health Guide for the Care and Use of Laboratory Animals.

Cannulation of mesenteric lymph and intraduodenal infusion tube

For these procedures, mice are placed under isoflurane anesthesia (induction at 5% and 2% maintenance during surgery), and both a mesenteric lymph duct cannula and duodenal infusion tube are installed. Prior to surgery, the mice are placed on a heated surgical pad. A surgical incision is made along the midline, and the abdominal viscera were manipulated with a retractor to expose the mesenteric lymph

duct. The duct is partially cut at the proximal end, and the catheter tip (micro-Renathane tubing cut on the bias to form a cannula tip; Braintree Scientific; catalog no.: MRE-025) was inserted at the outermost part of the duct and fastened with a drop of Krazy glue. For placement of the duodenal feeding tube, the stomach is exposed and drawn partially out of the abdominal cavity. We use an 18G needle to insert the micro-Renathane tubing (Braintree Scientific; catalog no.: MRE-037) into the stomach and just past the pyloric sphincter into the duodenum. This is secured with a purse-string suture. Using 5-0 suture, we closed the incision and placed the mouse in Snuggle restraint jacket (mouse Snuggle; Lomir, Inc, <https://maps.google.com/?q=213+West+Main+Street+Malone,+NY+12953&entry=gmail&source=g>; Malone, NY; MS02.5PM). Snuggled mice are placed on a rotator table in a temperature and humidity-controlled polyacrylic filter-top container (12" W × 14" L × 8" H). The externalized duodenal feeding tube is connected to a Harvard infusion pump. The externalized lymph catheter is carefully placed to allow gravity flow of lymph into Eppendorf collection tubes on ice. Mice stay in the chamber throughout the experiment. Postsurgery, mice continuously receive 5% glucose in saline, at a 0.3 ml/h infusion rate, via duodenal tube to compensate for fluid and electrolyte loss because of lymphatic drainage. The original Tso Lab 2-day lymph fistula model used postsurgery and overnight infusion of glucose/saline infusion to keep rats well hydrated (they cannot resorb the fluid lost in diverted lymph) (75). Because the mesenteric lymph is diverted, animals cannot be calorically replenished with lipids overnight; so instead glucose is preferable. Fluids must be infused via the intraduodenal infusion tube because the animals are restrained and cannot access water. In the Tso Lab protocol, rats are restrained in Bollman cages; in our protocol, mice are restrained with Snuggles. Either way, if the restraint is loosened enough for ad lib access to water, the animals will chew out their stitches and cannulas.

Lipid infusion and collection of hourly lymph

Mice are given a 300 μ l bolus (which takes 2–3 min to infuse the total volume), of lipid (SMOFlipid 20% lipid injectable emulsion; Fresenius Kabi AG) followed by continuous glucose/saline at 0.3 ml/h.

Choice of infusion TAG and amount. Each 100 ml of SMOFlipid 20% contains refined soybean oil (6.0 g), medium-chain TAG (6.0 g), refined olive oil (5.0 g), fish oil (3.0 g), purified egg phospholipids (1.2 g), all-rac- α -tocopherol (16–23 mg), glycerol (2.5 g), sodium oleate (30 mg), and sodium hydroxide to adjust pH. This test lipid is designed for clinical use in patients receiving intravenous parenteral nutrition. It contains lipids that are traditionally absorbed via both the lymphatic and portal route (refined soybean and olive oils and medium-chain TAG, respectively) (76). Lymph was collected on ice for 1 h prior to lipid infusion (which represents a “fasting” experimental time point) and then hourly for 6 h continuously after the bolus infusion. Weight of each hourly lymph samples was recorded and used for flow rate.

1-Day protocol. One hour prior (–1) to the bolus lipid infusion, mice received a continuous duodenal infusion of 5% glucose in sterile saline, and a single hour of “fasting” lymph is collected. At time 0, the continuous intraduodenal infusion is switched to a bolus infusion of 0.3 ml SMOFlipid (which

takes ~2–3 min to infuse). Immediately after the bolus lipid, the continuous glucose infusion is resumed. Lymph is then collected hourly on ice for 6 h after the bolus infusion. At 6 h, mice are euthanized, and tissues are collected.

2-Day protocol. In parallel with the 1-day mice, 2-day mice receive a continuous duodenal infusion of 5% glucose in sterile saline after the surgical implantation of both cannulas. The design branches at time 0, which would be the time for bolus lipid infusion in a 1-day model. Instead, 2-day mice continue to receive the continuous duodenal infusion of 5% glucose in sterile saline for the next ~18 h (through the overnight period). On the morning of the second day, a single hour of “fasting” lymph is collected. At this point, as in the 1-day model, at time 0, the continuous intraduodenal infusion is switched to a bolus infusion of 0.3 ml SMOLipid. Immediately after the bolus lipid, the continuous glucose infusion is resumed. Lymph is then collected hourly on ice for 6 h after the bolus infusion. At 6 h, mice are euthanized, and tissues are collected.

TAG assay. TAG concentrations were determined using TAG assay kit (Randox Laboratories Company, Crumlin, UK; catalog no.: TR210). Briefly, 2 µl of the diluted samples was incubated with 200 µl of enzyme reagent at 37°C for 5 min in a 96-well plate. The plate was read by MULTISKAN G0 (Thermo Fisher Scientific, Waltham, MA) plate reader at 500 nm. Standards and blanks were used for calculation of concentrations.

Flow cytometry

Cells from lymph collected prelipid and postlipid infusion were stained with antibodies on ice and protected from light. Intracellular staining was performed using the eBioscience Foxp3 staining kit as per the manufacturer’s instructions (Thermo Fisher Scientific; catalog no.: 00-5523-00). Cells were washed between each step using eBioscience™ Flow Cytometry Staining Buffer (Thermo Fisher Scientific; catalog no.: 00-4222-26). Flow cytometry samples were run at the University of Pittsburgh Flow Cytometry Core using a BD LSR II (Becton Dickson Biosciences) after appropriate compensation. Collected events were set at 100,000. Compensation controls using single stains were made using One Comp ebeads and UltraComp ebeads (eBioscience, Thermo Fisher Scientific; catalog no.: 01-3333-42) according to the manufacturer’s instructions. Automatic compensation was conducted by fluorescence-activated cell sorting Diva software. Fluorescence minus one control was used to determine appropriate gate positions at the same time of experimental preparation. Our gating strategy is summarized as follows (and in [supplemental Fig. S1](#)). When gating any sample, leukocytes were identified by forward scatter (FSC) area (FSC-A) by side

scatter area, followed by identification of single cells using FSC height by FSC width. Finally, live cells were gated on using FSC-A by Live/Dead viability dye (Near-IR Dead Cell Stain Kit; Thermo Fisher Scientific; catalog no.: L10119). The absence of the dye indicates live cells. Live cells were then identified as leukocytes using CD45 (BioLegend, San Diego, CA; catalog no.: 103106) by FSC-A and then further identified as helper T cells with CD4 (Thermo Fisher Scientific; catalog no.: 45-0042-82) by FSC-A. To distinguish naïve CD4 cells, CD4 was gated by CD25⁻ CD44^{low} CD62^{hi} (Thermo Fisher Scientific; catalog nos.: 25-0251-82, 48-0441-82, and 17-0621-82, respectively), and for Treg cells, CD4+ was gated by CD25⁺ Foxp3⁺ as double-positive cells. Fluorescence minus one controls were used to determine all gates except FSC by side scatter and single cells. When appropriate, Fc receptors were blocked using CD16/CD32 Monoclonal Antibody (Thermo Fisher Scientific; catalog no.: 14-0161-81), before staining with antimouse fluorochrome-conjugated antibodies FlowJo software (Treestar, Ashland, OR) was utilized for final analysis of collected data. Thermo Fisher Scientific and BioLegend antibodies used are described in [Table 1](#).

Statistics

Values are expressed as mean ± SEM. The differences between two groups were analyzed by Student’s *t* test, and the lymph flow rate and lymphatic TAG concentrations were analyzed by multiple unpaired *t* tests using GraphPad Prism 9 (GraphPad Software). Differences were considered statistically significant at *P* < 0.05.

RESULTS

Adapted the classic murine conscious lymph fistula model (6, 77–79) to a single day experimental design

In our 1-day surgical model, the implantation of double cannulas is immediately followed by duodenal lipid infusion for the delivery of dietary TAG directly to the small intestinal lumen (bypassing stomach emptying, pancreatic enzyme secretion, or bicarbonate buffering dysfunction that can occur in diseases of the small intestine (21, 80)).

The 1-day surgical model is summarized in [Fig. 1](#). Double cannulation takes approximately 2–4 h. Mice recover in Snuggle restraints and in a warmed and humidified incubator. One hour prior to the bolus lipid infusion, mice receive a continuous duodenal infusion of 5% glucose in sterile saline, and a single hour of “fasting” lymph is collected. The continuous

TABLE 1. Reagents used for flow cytometry analysis

Reagent	Catalog number	Source
CD4 monoclonal antibody (RM4-5), PerCP-Cyanine5.5, eBioscience™ (1:100 dilution)	45-0042-82	Thermo Fisher Scientific
CD25 monoclonal antibody (PC61.5), PE-Cyanine7 (1:250 dilution)	25-0251-82	Thermo Fisher Scientific
CD44 monoclonal antibody (IM7), eFluor 450, eBioscience™ (1:100 dilution)	48-0441-82	Thermo Fisher Scientific
CD62L (L-Selectin) Monoclonal Antibody (MEL-14), APC (1:400 dilution)	17-0621-82	Thermo Fisher Scientific
FOXP3 Monoclonal Antibody (FJK-16s), Alexa Fluor 488 (1:200 dilution)	53-5773-82	Thermo Fisher Scientific
LIVE/DEAD™ Fixable Near-IR Dead Cell Stain Kit	L10119	Thermo Fisher Scientific
eBioscience™ Foxp3/Transcription Factor Staining Buffer Set	00-5523-00	Thermo Fisher Scientific
eBioscience™ Flow Cytometry Staining Buffer	00-4222-26	Thermo Fisher Scientific
PE anti-mouse CD45 Antibody (1:200 dilution)	103106	BioLegend
CD16/CD32 Monoclonal Antibody, eBioscience™ (1:100 dilution)	14-0161-81	Thermo Fisher Scientific

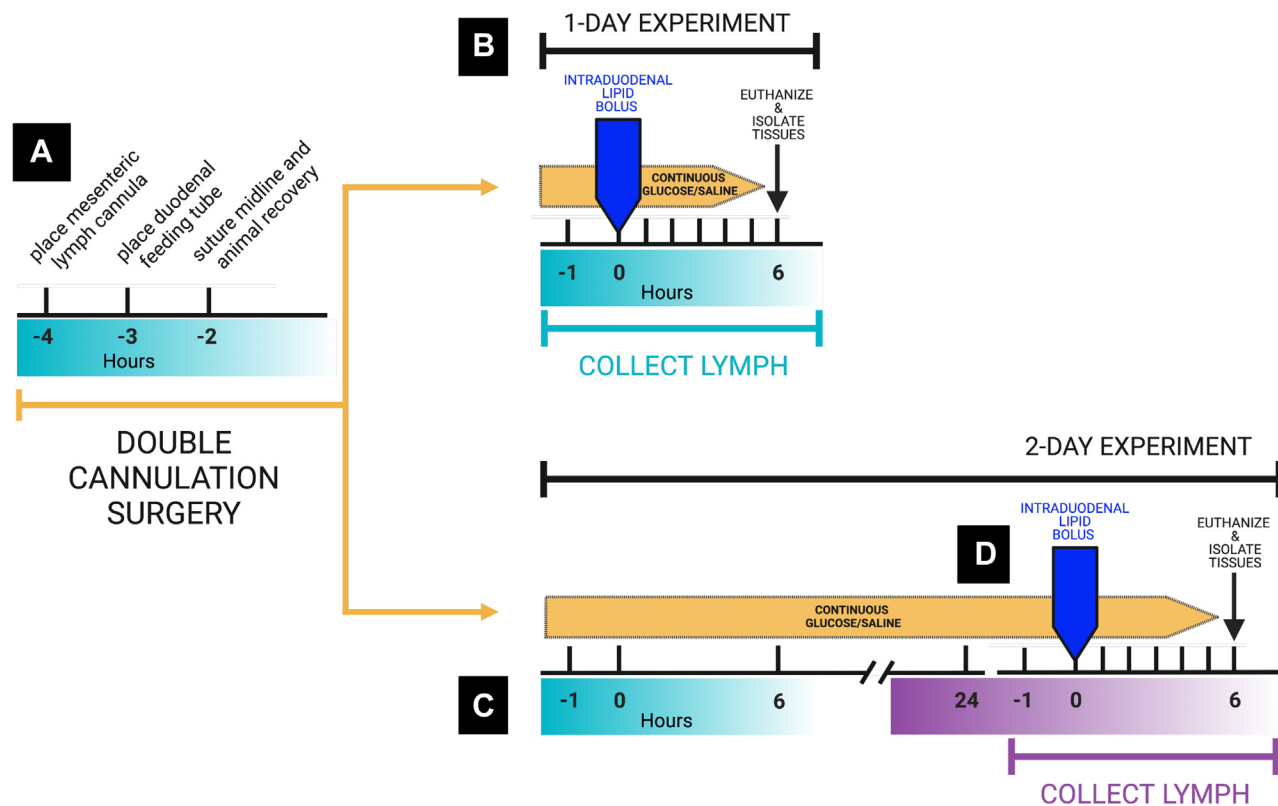


Fig. 1. Experimental model for 1-day versus 2-day lymph fistula mouse. **A:** Double cannulation takes approximately 2–4 h. Mice recover in Snuggle restraints and in a warmed incubator. **B:** One-day experimental model. One hour prior (–1) to the bolus lipid infusion, mice receive a continuous duodenal infusion of 5% glucose in sterile saline, and a single hour of “fasting” lymph is collected. At time 0, the continuous intraduodenal infusion is switched to a bolus infusion of 0.3 ml SMOFlipid. Immediately after the bolus lipid, the continuous glucose infusion is resumed. Lymph is collected hourly on ice for 6 h after the bolus infusion. At 6 h, mice are euthanized, and tissues were collected. **C:** Two-day experimental model. Mice receive a continuous duodenal infusion of 5% glucose in sterile saline as in (B), but the infusion continues for an additional ~18 h. **D:** On the morning of the second day, a single hour of “fasting” lymph is collected. As in (B), at time 0, the continuous intraduodenal infusion is switched to a bolus infusion of 0.3 ml SMOFlipid. Immediately after the bolus lipid, the continuous glucose infusion is resumed. Lymph is collected hourly on ice for 6 h after the bolus infusion. At 6 h, mice are euthanized, and tissues were collected. Created with BioRender.com.

intraduodenal infusion is then switched to a bolus infusion of 0.3 ml SMOFlipid. Immediately after the bolus lipid, the continuous glucose infusion is resumed. Lymph is collected on ice for 6 h continuously at 1-h intervals after the bolus infusion (for a total of six samples, each 1 h of lymph flow). **Figure 2** shows anatomical models and surgical photos of the 1-day technique.

This differs from the classic 2-day lymph fistula model by several points: 1) 2-day surgical model mice receive a continuous duodenal infusion of 5% glucose in sterile saline after surgeries until administration of lipid bolus the next day (overnight after cannula implantation); 2) mice that survive the overnight period then receive their bolus infusion of lipid (day 2) and lymph is then collected as in the 1-day surgical model; 3) the total duration of the experiment is reduced from 2 days to a single day.

Improved survival rates after 1-day surgical model design

Surgical success is considered a mouse that has milky lipid-rich flowing lymph starting ~15 min after the

duodenal lipid infusion and lasting at least 5 h. If an animal died prior to the start of the lipid infusion, or had no lymph flow after duodenal infusion, this qualifies as an experimental loss. We found that animals that underwent the 1-day surgical design had a 63.0% success rate, with 17 of 27 mice (**Fig. 3A**). In the classic 2-day surgical design, mice received the glucose/saline infusion immediately postsurgery and throughout an overnight recovery period. These mice received the duodenal lipid infusion on the morning of the second day. These mice were much more likely to die during the recovery period prior to the duodenal infusion, and they were more likely to lose steady lymph flow during either the glucose/saline infusion or in response to duodenal lipid. The success rate for this surgical design was 38.0% (8 of 21 mice), which is much lower than the 1-day model.

Comparison in lymph flow rates and total lymph secretion between 1-day and 2-day experimental models

We collected a 1 h of lymph flow from each mouse in the hour prior to duodenal lipid infusion (mice

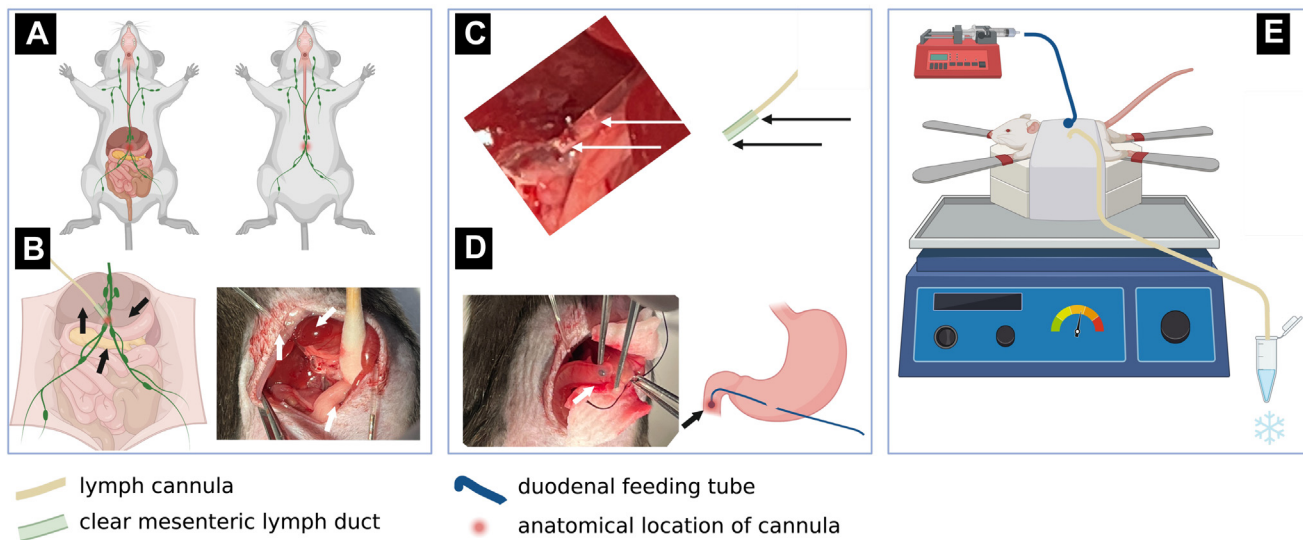


Fig. 2. Anatomical models and surgical photos for 1-day lymph fistula mouse. **A:** Cartoon mouse showing key areas of the liver and gastrointestinal tract and in green, the lymphatic vasculature. Red circle orients the site of the main mesenteric lymph duct and the focus on our surgical technique. **B:** The mesenteric lymph duct is found when the small intestine and liver are gently moved out of the body cavity. Black arrows in cartoon highlight key anatomical and surgical landmarks (clockwise from top of cartoon: liver, mesenteric fat, and clear cannula tubing). Photo shows the same anatomical and surgical landmarks as in cartoon but in white arrows. **C:** Higher magnification photo of the clear mesenteric cannula (upper white arrow), inserted into the mesenteric lymph duct (lower white arrow). Cartoon shows the mesenteric lymph cannula (upper black arrow, yellow tube) and clear mesenteric lymph duct (lower black arrow, green tube). **D:** Photo of the blue tip of the inserted duodenal feeding tube at ~5 cm into proximal duodenum. Cartoon shows the insertion of the duodenal feeding tube through the stomach wall, advanced ~5 cm into proximal duodenum. **E:** After implantation of duodenal and mesenteric lymph duct tubes, the midline incision is closed, and mice are placed in restraint snuggles on a warming pad on a gently rocking table. Fluid replenishment and test meals are delivered via an infusion pump through the intraduodenal feeding tube, and flowing mesenteric lymph is collected on ice in Eppendorf tubes. Cartoon legend is shown below figure. Created with [BioRender.com](https://www.biorender.com).

received the infusion of glucose/saline except during the 2–3 min lipid infusion), and then we collected hourly lymph samples for 6 h and kept lymph on ice. We found that the basal flow rate was not different between the two groups (Fig. 3B, time 0). Flow rates for both groups increased from 1 to 3 h after lipid infusion at the same rate. In rats, this increased lymph flow is a vagal response to duodenal lipid (81). Our data are the first to suggest that this occurs in mice as well as rats. Lymph flow rates only differ in the late postprandial period at hour 5 between groups (Fig. 3B, time 5). Overall, there is not a significant difference in the total amount (or volume) of lymph collected in 6 h between groups (Fig. 3C). This suggests that if mice survive the overnight recovery period, they can produce lymph volumes like their 1-day surgical model counterparts.

Increased TAG secretion in lymph in response to shortened experimental time

We measured lymphatic TAG concentrations following a bolus intraduodenal lipid infusion (Fig. 4A). In both groups, TAG secretion into lymph peaked at 3 h postlipid infusion. However, the magnitude of increase in TAG concentration is much higher in the 1-day compared with 2-day surgical model mice, and the 1-day mice secrete significantly more TAG into lymph than their 2-day counterparts over the entire course of lymph collection (Fig. 4B).

We wondered if the difference in TAG secretion could be attributed to the length of the recovery period because of the possibility that the long recovery period postsurgery diminishes small intestinal function. To test this possibility, we infused lipid and collected hourly lymph as in the 1-day design and followed this with an overnight recovery with continuous glucose/saline and a second lipid infusion on day 2 (experimental model depicted in Fig. 4D). Basal lymphatic TAG concentrations (0 h) were not different between the mice receiving their first or second lipid bolus, and after both bolus infusions, the lymphatic TAG peak at 3 h (Fig. 4C). Regardless of whether the mouse is receiving its second lipid bolus (as in Fig. 4C) or is receiving its first lipid bolus after an overnight recovery (as in first Fig. 4A), the magnitude of TAG in lymph is ~3× higher when the lipid infusion occurs on the first day than when it occurs on the second day. Therefore, the difference in TAG excursion is tied to length of time postsurgery, with 1-day lipid infusions resulting in higher lymphatic TAG concentrations.

Analysis of T lymphocytes in mesenteric lymph before and after a lipid bolus

Lymphocytes have been successfully isolated from ~5 μl static lymph and routinely from mesenteric lymph nodes (mLNs) but not from actively flowing lymph from mice receiving luminal nutrients (82–85).

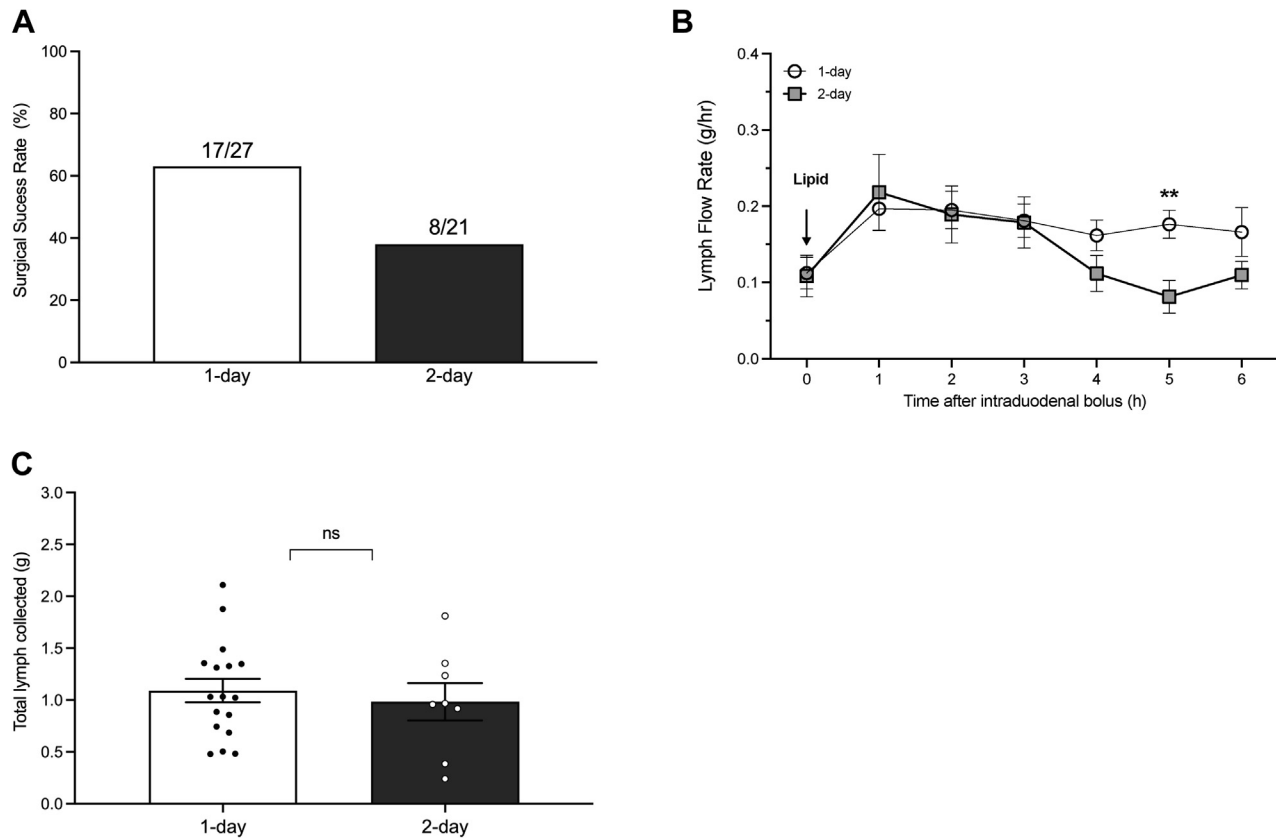


Fig. 3. Surgical success and lymph flow comparison between 1-day and 2-day surgical models. **A:** WT mice were fitted with an intraduodenal feeding tube and a mesenteric lymph cannula. Mice received a bolus infusion of 300 μ l of lipid. Surgical success resulted in the secretion of milky lipid-rich flowing lymph starting \sim 15 min after the duodenal lipid infusion and lasting at least 5 h. Data are plotted as the number of successful mice (1 day = 17 and 2 days = 8). $N = 48$. **B:** Hourly lymph flow rate in the 6 h after intraduodenal lipid infusion. In open circles, WT mice received lipid on the same day as surgery (1 day). In black squares, WT mice received lipid on second day after surgery (2 days). **C:** Total volume of lymph secreted by mice in each experimental paradigm. Values are means \pm SEM or means + SEM. $^{**}P < 0.005$.

Using our 1-day surgical model, mice received a continuous duodenal infusion of 5% glucose in sterile saline immediately after implantation of both cannulas, and then clear lymph was collected during this “pre-lipid bolus” period. At time 0, the continuous intraduodenal glucose/saline infusion is switched to a bolus infusion of 0.3 ml lipid. Immediately after the bolus of lipid, the continuous glucose infusion is resumed. “Postlipid bolus” lymph was then collected hourly on ice for 6 h continuously after the bolus infusion. Lymph was pooled from $n = 2$ –3 mice during each experiment to have enough cells for flow cytometry analysis, and the experiment was repeated three times.

Lymph (\sim 0.5 ml) was resuspended in 5 ml PBS, pelleted, and all cells were then stained with a CD4⁺ T-cell panel. As shown in Fig. 5A, \sim 3–4 million cells were present in 1 ml of lymph. Of these, 98–100% were CD45⁺ leukocytes (Fig. 5B) and 40–46% CD4⁺ cells (Fig. 5C). Of the total population of CD4⁺ cells, 77–84% were naïve CD4 cells (Fig. 5D), which had \sim 3–4% of CD4⁺CD25⁺Foxp3⁺ regulatory T cells (Fig. 5E). We found no significant differences between the populations of these cells in the prelipid versus postlipid

bolus groups (summarized in Fig. 5E). This analysis demonstrates the presence of CD45⁺ leukocytes, CD4⁺ and naïve CD4 cells, and regulatory T cells, and the similar lymphocyte populations in the prelipid and postlipid bolus lymph. In addition, the 1-day lymph fistula surgical model is appropriate for quantitative fluorescence-activated cell sorting immune profiling in a variety of experimental conditions.

DISCUSSION

The mouse lymph fistula technique should be considered the gold-standard technique for determining the partitioning of dietary nutrients into lymph in response to duodenal nutrients. It has been used to successfully uncover major mechanisms including the role of apolipoproteins, intestinal lipoproteins, lipid absorption, the secretion of incretin hormones into lymph in response to both lipids and glucose, and the relative absorption of xenobiotic toxins through the portal and lymphatic routes (4, 78, 53, 86–90). Our contribution to this technique is to 1) reduce the experimental time from 2 days to 1 day; 2) improve the

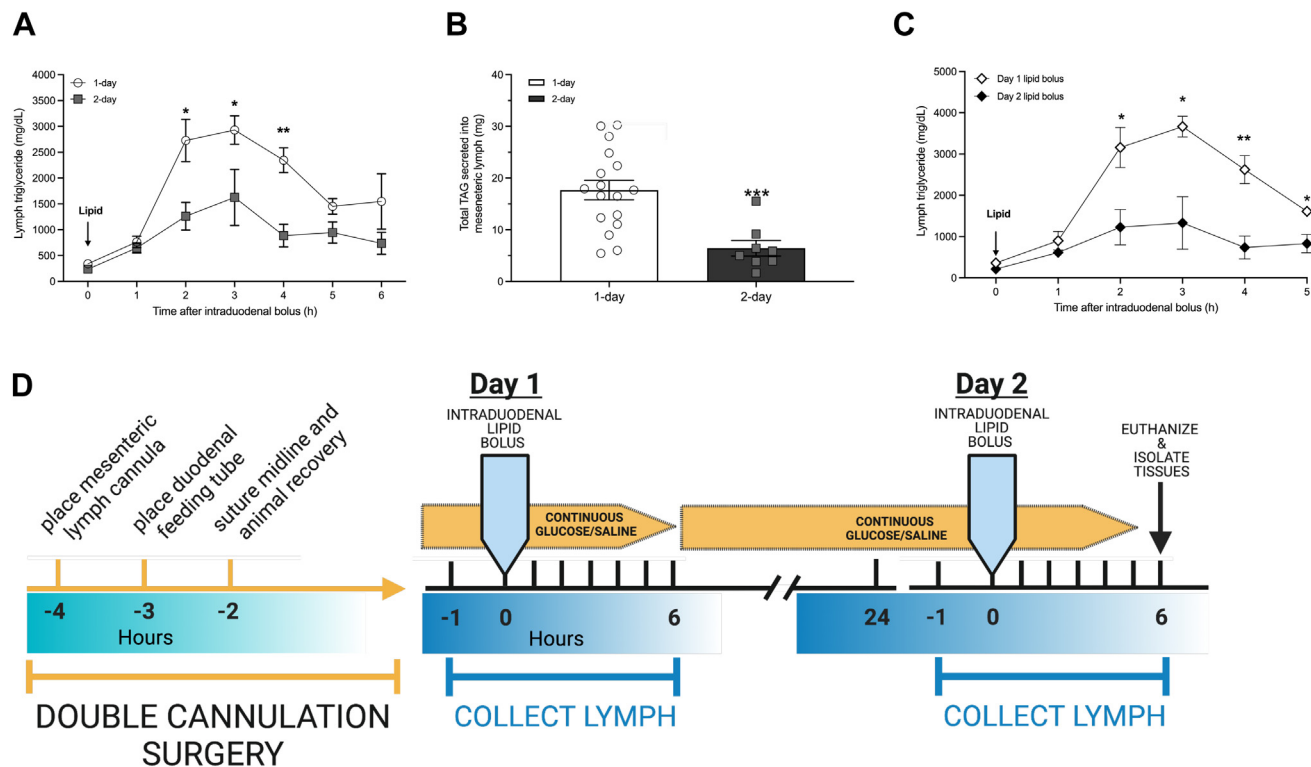


Fig. 4. Increased TAG secretion in lymph in response to shortened experimental time. **A:** In open circles, WT mice received intraduodenal lipid on the same day of surgery (1 day), $n = 17$. In black squares, WT mice received intraduodenal lipid after an overnight recovery period, on the day after surgery (2 days), $n = 8$. TAG concentrations in lymph in response to lipid bolus were determined by chemical assay. **B:** Total mass of TAG secreted during the 6 h after intraduodenal bolus. **C:** In white diamonds, WT mice received lipid on the same day as surgery (day 1). In black diamonds, the same mice received a second intraduodenal lipid dose the day after surgery—experimental model shown in (D). $n = 10+$, and values are means \pm SEM. $P < 0.05$ or means \pm SEM. * $P < 0.05$, ** $P < 0.005$, and *** $P < 0.0001$. Model created with [BioRender.com](https://www.biorender.com).

magnitude of duodenally infused lipids in lymph; 3) increase the reproducibility of the approach in mice; and 4) improve animal welfare; and 5) reduce the number of mice needed because of the higher survival rate.

A major experimental hurdle for collecting mesenteric lymph is the number of mice needed to ensure that enough mice survive the surgery and recover prior to and after lipid infusion. This is especially critical when using precious genetically modified mice and their WT littermates. By increasing the survival rate, we reduce the costs associated with both cohort generation and surgical labor. Our results show that the 1-day surgical model not only reduces the number of mice needed in each cohort but also reduces the amount of time the mice must survive after surgery (from ~ 24 to ~ 6 h). It had been thought that the overnight recovery period would let the animal to recover postoperative gastric contraction, reduce any “hang-over” anesthesia effects on lymph flow, and move the experimental period away from the immediate postsurgery recovery period (Dr Patrick Tso, unpublished communications and (77)). Our experiments actually test this assumption, and we find that the 24-h recovery period is not necessary for lymph flow and may paradoxically make

survival rates worse. This could be because recovery from major abdominal surgery cannot be achieved overnight and is fraught with risks of poor temperature regulation and hydration (in addition to the possibility that mice chew out their stitches or cannulas). Our updated surgical design reduces both unnecessary animal death and the potential for animal distress during this fragile postsurgical period. This supports a major goal of American Association for Accreditation of Laboratory Animal Care, which is animal “Replacement, Reduction, Refinement” (91).

We attribute increased survival not only to the reduction in surgical and experimental time but also to the use of alternative restraint after surgery. The lymph fistula technique has been primarily carried out in rats, which are restrained after surgery in Bollman restraint cages (70, 92). Both mice and rats move torsionally, even when their limbs are restrained, and they will rapidly and lethally chew out stitches and cannulas if not appropriately restrained. We have moved away from the Bollman restraint cage and instead used mouse Snuggles (which are essentially a soft restraint jacket) in both the 1-day and 2-day protocols described here. The Snuggles have two advantages: they keep the animals warm, and the mice are not

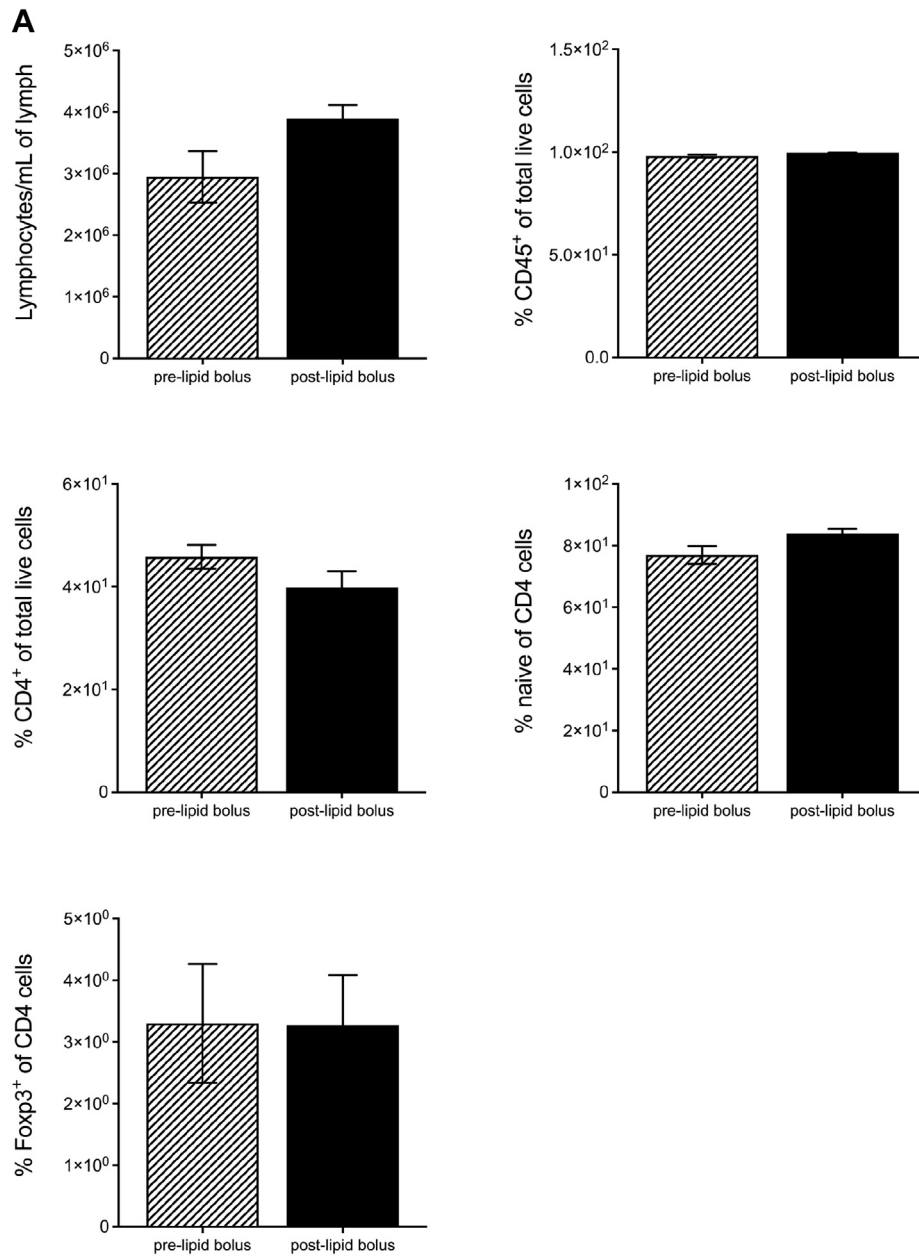


Fig. 5. Analysis of T lymphocytes in mesenteric lymph before and after a lipid bolus. WT mice were fitted with mesenteric lymph cannula and intraduodenal feeding tube. Mice then received a continuous duodenal infusion of 5% glucose in sterile saline. During this “prelipid bolus” period, clear lymph was collected. At time 0, the continuous intraduodenal infusion is switched to a bolus infusion of 0.3 ml lipid. Immediately after the bolus lipid, the continuous glucose infusion is resumed. “Postlipid bolus” lymph was then collected hourly on ice for 6 h after the bolus infusion. A: Number of cells per volume (1 ml) of lymph fluid collected and quantification of percent of parent population. Data are pooled from three independent experiments ($n = 2-3$ /experiment). B–E: Representative flow cytometric plots showing lymphocytes from equal volumes of prelipid or postlipid bolus lymph. Cells gated: Live lineage: negative for LIVE/DEAD stain, (B) total leukocyte: CD45⁺ cells gated on live cells, (C) CD4⁺ cell gated on CD45⁺ cells, (D) naïve CD4 cells: CD62^{hi} CD44^{low}, and (E) Treg cells: CD25⁺ Foxp3⁺ gated on CD4⁺. Numbers on plots denote cell frequencies (in percentages) of indicated parent populations and SEM, respectively. Data are representative examples of three independent experiments with $n = 2-3$ mice per experiment.

able to move torsionally. We believe this approach improves quality of life in the hours postsurgery and improves survival after the surgery.

TAG appearance in lymph represents a direct measure of the capacity and flux of enterocyte chylomicron secretion (since there is no removal mechanism for chylomicrons in this compartment—no lipases and

no tissue clearance mechanisms (53, 54)). The only way for chylomicrons to disappear from lymph is to enter the circulation at the thoracic duct. A fat tolerance test is often used as a proxy for dietary fat absorption capacity. If this is done in the presence of Poloxamer 407, it will block chylomicron metabolism and clearance by LPL and other lipid receptors in the circulation leading

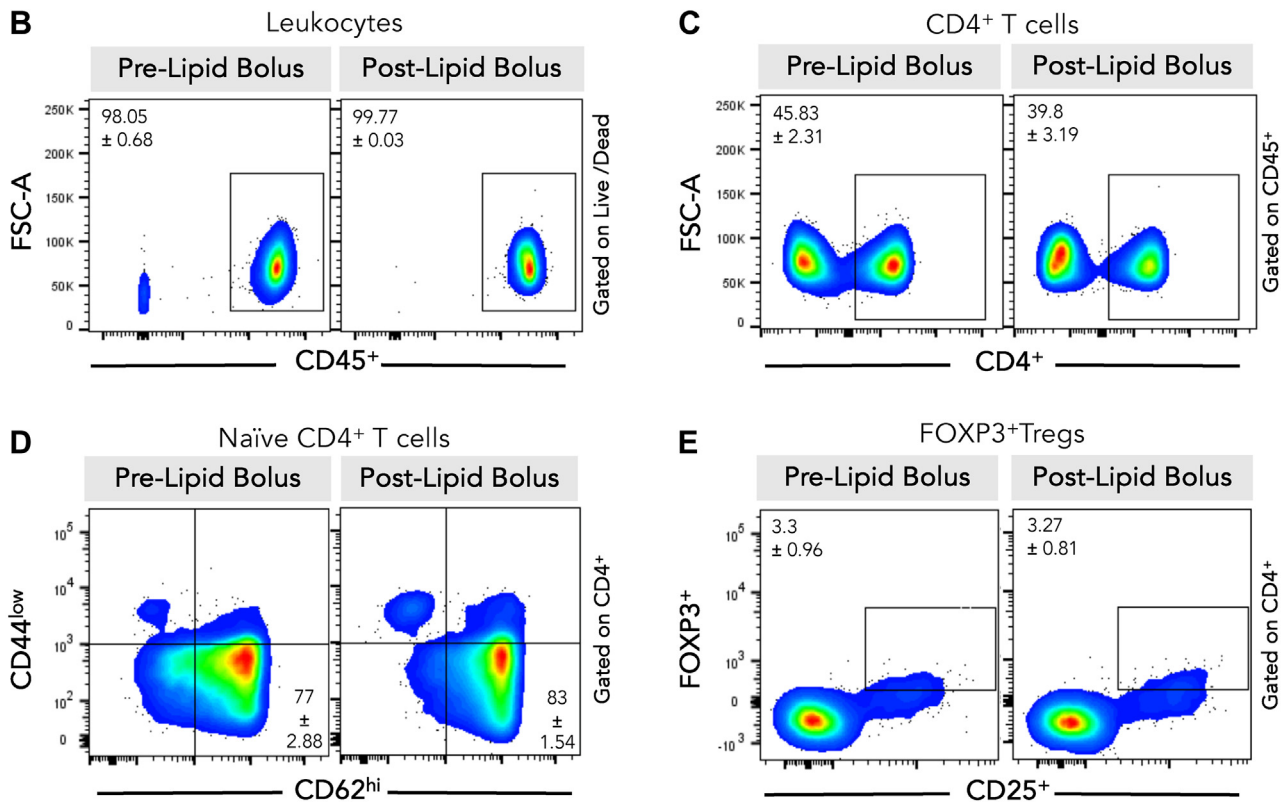


Fig. 5. (Continued).

to elevated plasma TAG coming from both liver and intestinal lipoproteins (93). This design cannot disentangle the kinetics of chylomicron metabolism from the metabolism of VLDLs in the absence of radiotracer and will not allow the isolation of naïve chylomicrons (since all the chylomicrons will be coated with poloxamer). Therefore, the mesenteric lymph is the most precise compartment for quantifying dietary lipid absorption and isolating chylomicrons.

Another advantage of isolating pure postlipid infusion mesenteric lymph is the ease with which chylomicrons can be isolated compared with from blood. We routinely ultracentrifuge lymph and simply collect the top creamy portion (53, 64, 94, 95). In postprandial lymph, this buoyant, density >1.006, fraction is almost all chylomicrons (63, 96). Mice secrete both apoB48 and apoB-100 on chylomicrons, whereas humans only make apoB-48 in the intestine, so we rarely use apoB-48 to differentiate murine lipoproteins (34). By comparison, isolating TAG-rich lipoproteins (chylomicrons and VLDL) from plasma is best done by tube slicing or differential centrifugation (69). In both cases, the chylomicron fraction will contain a heterogeneous mixture of chylomicrons, chylomicron remnants, and VLDL.

We and others have a significant interest in intestinal immune cells, including those with the potential to travel between the gut and circulation. The lymphatic niche is also an essential barrier to the movement of

enteric pathogens throughout the body. We undertook a basic analysis of T-cell populations and did not focus on specific effect/memory T-cell subsets. Our data show that those analyses would be possible in the future. That we find no differences in T-cell populations in prelipid and postlipid bolus lymph could be due to a lack of granularity, since we analyzed a single mixed sample made up of 6 h of postlipid bolus lymph (rather than individually analyzing each hour of lymph). Because of the reasonable volume of lymph collected each hour, these analyses would be possible in the future. Despite this, we would not expect huge differences in T-cell populations, since mesenteric lymph is cannulated after the lymph leaves the mLNs. Any immune cells that are trafficking between the lamina propria and the mLN or vice versa would not be present in this postnodal lymph, though naïve cells would be present. This supports the role of the mLN as the final mucosal firewall between activated immune cells or bacterial translocation and peripheral tissues (97–99). The mLN firewall is critical because escape of antigen-presenting cells from the gut into the circulation would stimulate naïve extraintestinal immune cells to respond to mucosal antigens (dietary, microbial, and self). The result would be highly inflammatory effector immune cells trafficking to the site of those antigens (the gut), which would result in autoimmune disorders like Crohn's disease and ulcerative colitis. Our model is a unique biological site where appropriate versus

defective immune cell dynamics can be measured, and the postnodal lymph compartment could be a rich source of information about the inflammatory state of the mucosa in many diseases.

In addition to chylomicrons, the small intestine also secretes HDLs, fat soluble-vitamins, and antigen from commensal microorganisms. It is intriguing to speculate that comparisons of lymphocyte populations, specialized lipids, antigens, and gut hormones, in postnodal flowing lymph versus the blood compartment could reveal dynamics of intestinal immunity and mucosal barrier function, nutrient processing, and dysfunction in these processes during metabolic disease. We propose this 1-day lymph fistula model as a valuable tool for directly measuring these processes and show for the first time that these analyses are possible with the 1-day lymph fistula mouse model.

Data Availability

Raw data are housed on the Kohan Lab server at the University of Pittsburgh School of Medicine. Data will be shared upon request to the corresponding author: Alison B. Kohan, PhD, University of Pittsburgh School of Medicine; Email: akohan@pitt.edu. 

Supplemental Data

This article contains [supplemental data](#).

Acknowledgments

Dr Kohan personally thank Dr Patrick Tso, a leader and innovator in the study of dietary lipid absorption, metabolism, and lymph. He recently retired after 40+ years as one of the world's leading experts in these areas. Dr Tso taught his mentees to ask clinically important questions and communicate the importance of our findings. He modeled being both a parent and a scientist. Dr Tso is universally known as both generous and collaborative. Many of his mentees have paid forward this generosity and are passing on these ideals to a next generation of trainees. Thank you. The authors also thank Leandra K. Gardner (BS, Division of Endocrinology and Metabolism, Department of Medicine, University of Pittsburgh) for providing photos of surgical technique.

Author Contributions

A. B. K. conceptualization; N. D. methodology; N. D. validation; L. T. and J. S. K. formal analysis; N. D. and L. T. investigation; N. D. resources; L. T. and J. S. K. data curation; A. B. K. writing—original draft; N. D. writing—review & editing; L. T. and J. S. K. visualization; A. B. K. supervision; A. B. K. project administration; A. B. K. funding acquisition.

Author ORCIDs

Alison B. Kohan  <https://orcid.org/0000-0003-3127-7283>

Funding and Additional Information

The authors are extremely grateful to the Cystic Fibrosis Foundation (Pilot and Feasibility Award 1810; to A. B. K.),

the Rainin Foundation (Synergy Award, to principal investigator G. J. Randolph and coinvestigator A. B. K.), and the National Institutes of Health (grant nos.: R01DK118239 and R03DK116011; to A. B. K.) for their support of these studies. The content is solely the responsibility of the authors and does not necessarily represent the official views of the National Institutes of Health.

Conflict of Interest

The authors declare that they have no conflicts of interest with the contents of this article.

Abbreviations

FSC, forward scatter; FSC-A, forward scatter area; LPS, lipopolysaccharide; mLN, mesenteric lymph node; TAG, triglyceride.

Manuscript received June 10, 2022, and in revised form September 15, 2022. Published, JLR Papers in Press, September 21, 2022, <https://doi.org/10.1016/j.jlr.2022.100284>

REFERENCES

1. Kindel, T., Lee, D. M., and Tso, P. (2010) The mechanism of the formation and secretion of chylomicrons. *Atheroscler. Suppl.* **11**, 11–1616
2. Mansbach, C. M., and Siddiqi, S. A. (2010) The biogenesis of chylomicrons. *Annu. Rev. Physiol.* **72**, 315–333
3. Giammanco, A., Cefalù, A. B., Noto, D., and Averna, M. R. (2015) The pathophysiology of intestinal lipoprotein production. *Front. Physiol.* **6**, 1–10
4. Tso, P., and Balint, J. A. (1986) Formation and transport of chylomicrons by enterocytes to the lymphatics. *Am. J. Physiol.* **250**, G715–G726
5. Ooi, E., Watts, G., Ng, T., and Barrett, P. (2015) Effect of dietary fatty acids on human lipoprotein metabolism: a comprehensive update. *Nutrients* **7**, 4416–4425
6. Kohan, A. B., Howles, P. N., and Tso, P. (2012) Methods for studying rodent intestinal lipoprotein production and metabolism. *Curr. Protoc. Mouse Biol.* **2**, 219–230
7. Tso, P., Drake, D. S., Black, D. D., and Sabesin, S. M. (1984) Evidence for separate pathways of chylomicron and very low-density lipoprotein assembly and transport by rat small intestine. *Am. J. Physiol.* **247**, G599–G610
8. Ockner, R. K., Hughes, F. B., and Isselbacher, K. J. (1969) Very low density lipoproteins in intestinal lymph: role in triglyceride and cholesterol transport during fat absorption. *J. Clin. Invest.* **48**, 2367–2373
9. Risser, T. R., Reaven, G. M., and Reaven, E. P. (1978) Intestinal contribution to secretion of very low density lipoproteins into plasma. *Am. J. Physiol. Endocrinol. Metab. Gastrointest. Physiol.* **3**, 277–281
10. Nutting, D., Hall, J., Barrowman, J. A., and Tso, P. (1989) Further studies on the mechanism of inhibition of intestinal chylomicron transport by Pluronic L-81. *Biochim. Biophys. Acta.* **1004**, 357–362
11. Hugh, P., and Barrett, R. (1998) Kinetics of triglyceride rich lipoproteins: chylomicrons and very low density lipoproteins. *Atherosclerosis.* **141**, S35–S40
12. Stahel, P., Xiao, C., Davis, X., Tso, P., and Lewis, G. F. (2019) Glucose and GLP-2 (Glucagon-Like Peptide-2) mobilize intestinal triglyceride by distinct mechanisms. *Arterioscler. Thromb. Vasc. Biol.* **39**
13. Turner, M. W., Frase, S., and Mansbach 2nd, C. M. (1988) Isolation of the early phase of chylomicron formation in intestinal epithelial cells of rats. *Biochimie.* **70**, 1263–1268
14. Shiau, Y-F., Popper, D. A., Reed, M., Umstetter, C., Capuzzi, D., and Levine, G. M. (1985) Intestinal triglycerides are derived from both endogenous and exogenous sources. *Am. J. Physiol.* **248**, G164–G169

15. Hayashi, H., Fujimoto, K., Cardelli, J. A., Nutting, D. F., Bergstedt, S., and Tso, P. (1990) Fat feeding increases size, but not number, of chylomicrons produced by small intestine. *Am. J. Physiol.* **259**, G709–G719
16. Tso, P., Lindstrom, M. B., and Borgstrom, B. (1987) Factors regulating the formation of chylomicrons and very-low-density lipoproteins by the rat small intestine. *Biochim. Biophys. Acta.* **922**, 304–313
17. Gangl, A., and Ockner, R. K. (1975) Intestinal metabolism of plasma free fatty acids. Intracellular compartmentation and mechanisms of control. *J. Clin. Invest.* **55**, 803–813
18. Duez, H., Lamarche, B., Uffelman, K. D., Valero, R., Cohn, J. S., and Lewis, G. F. (2006) Hyperinsulinemia is associated with increased production rate of intestinal apolipoprotein B-48-containing lipoproteins in humans. *Arterioscler. Thromb. Vasc. Biol.* **26**, 1357–1363
19. Taghibiglou, C., Carpentier, A., Van Iderstine, S. C., Chen, B., Rudy, D., Aiton, A., *et al.* (2000) Mechanisms of hepatic very low density lipoprotein overproduction in insulin resistance. Evidence for enhanced lipoprotein assembly, reduced intracellular ApoB degradation, and increased microsomal triglyceride transfer protein in a fructose-fed hamster model. *J. Biol. Chem.* **275**, 8416–8425
20. Jung, H. R., Turner, S. M., Neese, R. A., Young, S. G., and Hellerstein, M. K. (1999) Metabolic adaptations to dietary fat malabsorption in chylomicron-deficient mice. *Biochem. J.* **343**, 473–478
21. Wouthuyzen-Bakker, M., Bodewes, F. A. J. A., and Verkade, H. J. (2011) Persistent fat malabsorption in cystic fibrosis; lessons from patients and mice. *J. Cyst. Fibros.* **10**, 150–158
22. Chuang, J. C., Lopez, A. M., and Turley, S. D. (2017) Quantitation of the rates of hepatic and intestinal cholesterol synthesis in lysosomal acid lipase-deficient mice before and during treatment with ezetimibe. *Biochem. Pharmacol.* **135**, 116–125
23. Assadollahi, F., Cavallero, E., Buxtorf, J. C., Jacotot, B., and Beaumont, J. L. (1994) Familial xanthomatous hypercholesterolemia: abnormal exogenous lipid metabolism evidenced by the vitamin A test. *Ann. Nutr. Metab.* **38**, 307–312
24. Reiner, Z., Guardamagna, O., Nair, D., Soran, H., Hovingh, K., Bertolini, S., *et al.* (2014) Lysosomal acid lipase deficiency—an under-recognized cause of dyslipidaemia and liver dysfunction. *Atherosclerosis.* **235**, 21–30
25. Pisciotta, L., Tozzi, G., Travaglini, L., Taurisano, R., Lucchi, T., Indolfi, G., *et al.* (2017) Molecular and clinical characterization of a series of patients with childhood-onset lysosomal acid lipase deficiency. Retrospective investigations, follow-up and detection of two novel LIPA pathogenic variants. *Atherosclerosis.* **265**, 124–132
26. Watt, M. J., Clark, A. K., Selth, L. A., Haynes, V. R., Lister, N., Rebello, R., *et al.* (2019) Suppressing fatty acid uptake has therapeutic effects in preclinical models of prostate cancer. *Sci. Transl. Med.* **11**, eaau5758
27. Nauli, A. M., Nassir, F., Zheng, S., Yang, Q., Lo, C. M., Vonlehmden, S. B., *et al.* (2006) CD36 is important for chylomicron formation and secretion and may mediate cholesterol uptake in the proximal intestine. *Gastroenterology.* **131**, 1197–1207
28. Hussain, M. M., Shi, J., and Dreizen, P. (2003) Microsomal triglyceride transfer protein and its role in apoB-lipoprotein assembly. *J. Lipid Res.* **44**, 22–32
29. Pan, X., and Hussain, M. M. (2012) Gut triglyceride production. *Biochim. Biophys. Acta.* **1821**, 727–735
30. Zhang, L. J., Wang, C., Yuan, Y., Wang, H., Wu, J., Liu, F., *et al.* (2014) Cideb facilitates the lipidation of chylomicrons in the small intestine. *J. Lipid Res.* **55**, 1279–1287
31. Jaschke, A., Chung, B., Hesse, D., Kluge, R., Zahn, C., Moser, M., *et al.* (2012) The GTPase ARFRP1 controls the lipidation of chylomicrons in the Golgi of the intestinal epithelium. *Hum. Mol. Genet.* **21**, 3128–3142
32. Storch, J., Zhou, Y. X., and Lagakos, W. S. (2008) Metabolism of apical versus basolateral sn-2-monoacylglycerol and fatty acids in rodent small intestine. *J. Lipid Res.* **49**, 1762–1769
33. Mansbach 2nd, C. M. (1977) The origin of chylomicron phosphatidylcholine in the rat. *J. Clin. Invest.* **60**, 411–420
34. Lo, C. M., Nordskog, B. K., Nauli, A. M., Zheng, S., Vonlehmden, S. B., Yang, Q., *et al.* (2008) Why does the gut choose apolipoprotein B48 but not B100 for chylomicron formation? *Am. J. Physiol. Gastrointest. Liver Physiol.* **294**, G344–G352
35. Hirano, K., Young, S. G., Farese, R. V., Ng, J., Sande, E., Warburton, C., *et al.* (1996) Targeted disruption of the mouse apobec-1 gene abolishes apolipoprotein B mRNA editing and eliminates apolipoprotein B48. *J. Biol. Chem.* **271**, 9887–9890
36. Lo, C. C., and Coschigano, K. T. (2020) ApoB48 as an efficient regulator of intestinal lipid transport. *Front. Physiol.* **11**, 796
37. Wang, C. S., McConathy, W. J., Kloer, H. U., and Alaupovic, P. (1985) Modulation of lipoprotein lipase activity by apolipoproteins. Effect of apolipoprotein C-III. *J. Clin. Invest.* **75**, 384–390
38. Gordts, P. L. S. M., Nock, R., Son, N. H., Ramms, B., Lew, I., Gonzales, J. C., *et al.* (2016) ApoC-III inhibits clearance of triglyceride-rich lipoproteins through LDL family receptors. *J. Clin. Invest.* **126**, 2855–2866
39. Goldberg, I. J., Scheraldi, C. A., Yacoub, L. K., Saxena, U., and Bisgaier, C. L. (1990) Lipoprotein ApoC-II activation of lipoprotein lipase. Modulation by apolipoprotein A-IV. *J. Biol. Chem.* **265**, 4266–4272
40. Rensen, P. C., and van Berkel, T. J. (1996) Apolipoprotein E effectively inhibits lipoprotein lipase-mediated lipolysis of chylomicron-like triglyceride-rich lipid emulsions in vitro and in vivo. *J. Biol. Chem.* **271**, 14791–14799
41. Pollin, T. I. T., Damcott, C. M., Shen, H., Ott, S. H., Shelton, J., Horenstein, R. B., *et al.* (2008) A null mutation in human APOC3 confers a favorable plasma lipid profile and apparent cardioprotection. *Science.* **322**, 1702–1705
42. Ito, Y., Azrolan, C., O'Connell, A., Walsh, A., and Breslow, J. (1990) Hypertriglyceridemia as a result of human apo CIII gene expression in transgenic mice. *Science.* **249**, 790–793
43. TG and HDL Working Group of the Exome Sequencing Project, National Heart, Lung, and Blood Institute, Crosby, J., Peloso, G. M., Auer, P. L., Crosslin, D. R., Stitzel, N. O., *et al.* (2014) Loss-of-function mutations in *APOC3*, triglycerides, and coronary disease. *N. Engl. J. Med.* **371**, 22–31
44. Jørgensen, A. B., Frikke-Schmidt, R., Nordestgaard, B. G., and Tybjaerg-Hansen, A. (2014) Loss-of-function mutations in *APOC3* and risk of ischemic vascular disease. *N. Engl. J. Med.* **371**, 32–41
45. Amar, M. J., Sakurai, T., Sakurai-Ikuta, A., Sviridov, D., Freeman, L., Ahsan, L., *et al.* (2015) A novel apolipoprotein C-II mimetic peptide that activates lipoprotein lipase and decreases serum triglycerides in apolipoprotein E-knockout mice. *J. Pharmacol. Exp. Ther.* **352**, 227–235
46. Sakurai, T., Sakurai, A., Vaisman, B. L., Amar, M. J., Liu, C., Gordon, S. M., *et al.* (2016) Creation of Apolipoprotein C-II (ApoC-II) mutant mice and correction of their hypertriglyceridemia with an ApoC-II mimetic peptide. *J. Pharmacol. Exp. Ther.* **356**, 341–353
47. Park, H. J., Lee, S., Park, C. M., Yoo, K., and Seo, J. M. (2021) Reversal of intestinal failure-associated liver disease by increasing fish oil in a multi-oil intravenous lipid emulsion in adult short bowel-syndrome patients. *J. Parenter. Enter. Nutr.* **45**, 204–207
48. Machigashira, S., Kaji, T., Onishi, S., Yano, K., Harumatsu, T., Yamada, K., *et al.* (2021) What is the optimal lipid emulsion for preventing intestinal failure-associated liver disease following parenteral feeding in a rat model of short-bowel syndrome? *Pediatr. Surg. Int.* **37**, 247–256
49. Molinos, N., Akimov, O., Santos, C. S., Markley, M., Adigun, A., Duro, D., *et al.* (2021) Reversal of intestinal failure-associated liver disease in an infant treated with mixed lipid emulsion and multidisciplinary intestinal rehabilitation program. *J. Parenter. Enter. Nutr.* **45**, 844–847
50. Hultin, M., Carneheim, C., Rosenqvist, K., and Olivecrona, T. (1995) Intravenous lipid emulsions: removal mechanisms as compared to chylomicrons. *J. Lipid Res.* **36**, 2174–2184
51. Kortz, W. J., Schirmer, B. D., Mansbach, C. M., Shelburne, F., Togli, M. R., and Quarfordt, S. H. (1984) Hepatic uptake of chylomicrons and triglyceride emulsions in rats fed diets of differing fat content. *J. Lipid Res.* **25**, 799–804
52. Mansbach 2nd, C. M., Arnold, A., and Cox, M. A. (1985) Factors influencing triacylglycerol delivery into mesenteric lymph. *Am. J. Physiol.* **249**, G642–G648
53. Wang, F., Kohan, A. B., Dong, H. H., Yang, Q., Xu, M., Huesman, S., *et al.* (2014) Overexpression of apolipoprotein C-III decreases secretion of dietary triglyceride into lymph. *Physiol. Rep.* **2**, e00247
54. Spiller, R. C., Trotman, I. F., Adrian, T. E., Bloom, S. R., Misiewicz, J. J., and Silk, D. B. (1988) Further characterisation of

- the 'ileal brake' reflex in man—effect of ileal infusion of partial digests of fat, protein, and starch on jejunal motility and release of neurotensin, enteroglucagon, and peptide YY. *Gut*. **29**, 1042–1051
55. Wang, Y., Ghoshal, S., Ward, M., de Villiers, W., Woodward, J., and Eckhardt, E. (2009) Chylomicrons promote intestinal absorption and systemic dissemination of dietary antigen (Ovalbumin) in mice. *PLoS One* **4**, e8442
 56. Ebara, T., Ramakrishnan, R., Steiner, G., and Shachter, N. S. (1997) Chylomicronemia due to apolipoprotein CIII overexpression in apolipoprotein E-null mice. Apolipoprotein CIII-induced hypertriglyceridemia is not mediated by effects on apolipoprotein E. *J. Clin. Invest.* **99**, 2672–2681
 57. Goldberg, I. J., Eckel, R. H., and McPherson, R. (2011) Triglycerides and heart disease: still a hypothesis? *Arterioscler. Thromb. Vasc. Biol.* **31**, 1716–1725
 58. Gao, Y., Nelson, D. W., Banh, T., Yen, M. I., and Yen, C. L. E. (2013) Intestine-specific expression of MOGAT2 partially restores metabolic efficiency in Mogat2-deficient mice. *J. Lipid Res.* **54**, 1644–1652
 59. Wang, F., Kohan, A. B., Lo, C. M., Liu, M., Howles, P., and Tso, P. (2015) Apolipoprotein A-IV: a protein intimately involved in metabolism. *J. Lipid Res.* **56**, 1403–1418
 60. Windler, E., Chao, Y., and Havel, R. J. (1980) Determinants of hepatic uptake of triglyceride-rich lipoproteins and their remnants in the rat. *J. Biol. Chem.* **255**, 5475–5480
 61. Mansbach 2nd, C. M., and Dowell, R. F. (1995) Role of the intestine in chylomicron remnant clearance. *Am. J. Physiol.* **269**, G144–G152
 62. Aalto-Seifälä, K., Weinstock, P. H., Bisgaier, C. L., Wu, L., Smith, J. D., and Breslow, J. L. (1996) Further characterization of the metabolic properties of triglyceride-rich lipoproteins from human and mouse apoC-III transgenic mice. *J. Lipid Res.* **37**, 1802–1811
 63. Kohan, A. B., Qing, Y., Cyphert, H. A., Tso, P., and Salati, L. M. (2011) Chylomicron remnants and nonesterified fatty acids differ in their ability to inhibit genes involved in lipogenesis in rats. *J. Nutr.* **141**, 171–176
 64. Li, D., Rodia, C. N., Johnson, Z. K., Bae, M., Muter, A., Heussinger, A. E., et al. (2019) Intestinal basolateral lipid substrate transport is linked to chylomicron secretion and is regulated by apoC-III. *J. Lipid Res.* **60**, 1503–1515
 65. Jattan, J., Rodia, C., Li, D., Diakhate, A., Dong, H., Bataille, A., et al. (2017) Using primary murine intestinal enteroids to study dietary TAG absorption, lipoprotein synthesis, and the role of apoC-III in the intestine. *J. Lipid Res.* **58**, 853–865
 66. Soayfane, Z., Tercé, F., Cantiello, M., Robenek, H., Nauze, M., Bézirard, V., et al. (2016) Exposure to dietary lipid leads to rapid production of cytosolic lipid droplets near the brush border membrane. *Nutr. Metab. (Lond)*. **13**, 48
 67. Morton, A. M., Furtado, J. D., Lee, J., Amerine, W., Davidson, M. H., and Sacks, F. M. (2016) The effect of omega-3 carboxylic acids on apolipoprotein CIII-containing lipoproteins in severe hypertriglyceridemia. *J. Clin. Lipidol.* **10**, 1442–1451.e4
 68. Hirasawa, A., Tsumaya, K., Awaji, T., Katsuma, S., Adachi, T., Yamada, M., et al. (2005) Free fatty acids regulate gut incretin glucagon-like peptide-1 secretion through GPR120. *Nat. Med.* **11**, 90–94
 69. Redgrave, T. G., Roberts, D. C., and West, C. E. (1975) Separation of plasma lipoproteins by density-gradient ultracentrifugation. *Anal. Biochem.* **65**, 42–49
 70. Bollman, J. L., Cain, J. C., and Grindlay, J. H. (1948) Techniques for the collection of lymph from the liver, small intestine, or thoracic duct of the rat. *J. Lab. Clin. Med.* **33**, 1349–1352
 71. Milasan, A., Dallaire, F., Mayer, G., and Martel, C. (2016) Effects of LDL Receptor Modulation on Lymphatic Function. *Sci. Rep.* **6**
 72. Zawieja, D. C., Thangaswamy, S., Wang, W., Furtado, R., Clement, C. C., Papadopoulos, Z., et al. (2019) Lymphatic cannulation for lymph sampling and molecular delivery. *J. Immunol.* **203**, 2339–2350
 73. Clement, C. C., and Santambrogio, L. (2013) The lymph self-antigen repertoire. *Front. Immunol.* **4**
 74. Arpaia, N., Campbell, C., Fan, X., Dikiy, S., van der Veeken, J., deRoos, P., et al. (2013) Metabolites produced by commensal bacteria promote peripheral regulatory T-cell generation. *Nature*. **504**, 451–455
 75. Kohan, A. B., Yoder, S. M., and Tso, P. (2011) Using the lymphatics to study nutrient absorption and the secretion of gastrointestinal hormones. *Physiol. Behav.* **105**, 82–88
 76. Fernandez, M. L., and West, K. L. (2005) Mechanisms by which dietary fatty acids modulate plasma lipids. *J. Nutr.* **135**, 2075–2078
 77. Kohan, A., Yoder, S., and Tso, P. (2010) Lymphatics in intestinal transport of nutrients and gastrointestinal hormones. *Ann. N. Y. Acad. Sci.* **1207**, E44–E51
 78. Jandacek, R. J., and Tso, P. (2008) Organochlorine compounds are absorbed via lymph and portal circulation. *FASEB J.* **22**
 79. Anzai, K., Fukagawa, K., Iwakiri, R., Fujimoto, K., Akashi, K., and Tso, P. (2009) Increased lipid absorption and transport in the small intestine of Zucker obese rats. *J. Clin. Biochem. Nutr.* **45**, 82–85
 80. Hunt, J. N., and Knox, M. T. (1968) A relation between the chain length of fatty acids and the slowing of gastric emptying. *J. Physiol.* **194**, 327–336
 81. Kalogeris, T. J., Holden, V. R., and Tso, P. (1999) Stimulation of jejunal synthesis of apolipoprotein A-IV by ileal lipid infusion is blocked by vagotomy. *Am. J. Physiol.* **277**, G1081–G1087
 82. Ivanov, S., Scallan, J. P., Kim, K. W., Werth, K., Johnson, M. W., Saunders, B. T., et al. (2016) CCR7 and IRF4-dependent dendritic cells regulate lymphatic collecting vessel permeability. *J. Clin. Invest.* **126**, 1581–1591
 83. Ormai, S., and Palkovits, M. (1972) Size distribution of lymphocytes in the thoracic duct lymph in rat after lymphocyte mobilization induced by polymethacrylic acid. *Blut.* **24**, 161–165
 84. Galkowska, H., and Olszewski, W. L. (1992) Immune events in skin. I. Spontaneous cluster formation of dendritic (Veiled) cells and lymphocytes from skin lymph. *Scand. J. Immunol.* **35**, 727–734
 85. Trevaskis, N. L., Hu, L., Caliph, S. M., Han, S., and Porter, C. J. H. (2015) The mesenteric lymph duct cannulated rat model: application to the assessment of intestinal lymphatic drug transport. *J. Vis. Exp.* **6**, 52389
 86. Lu, W. J., Yang, Q., Sun, W., Woods, S. C., D'Alessio, D., and Tso, P. (2007) The regulation of the lymphatic secretion of glucagon-like peptide-1 (GLP-1) by intestinal absorption of fat and carbohydrate. *Am. J. Physiol. Gastrointest. Liver Physiol.* **293**, G963–G971
 87. Hayashi, H., Nutting, D. F., Fujimoto, K., Cardelli, J. A., Black, D., and Tso, P. (1990) Transport of lipid and apolipoproteins A-I and A-IV in intestinal lymph of the rat. *J. Lipid Res.* **31**, 1613–1625
 88. Wu, A. L., and Windmueller, H. G. (1978) Identification of circulating apolipoproteins synthesized by rat small intestine in vivo. *J. Biol. Chem.* **253**, 2525–2528
 89. Jandacek, R. J., Rider, T., Keller, E. R., and Tso, P. (2010) The effect of olestra on the absorption, excretion and storage of 2,2', 5,5' tetrachlorobiphenyl; 3,3',4,4' tetrachlorobiphenyl; and perfluorooctanoic acid. *Env. Int.* **36**, 880–883
 90. Guo, Q., Avramoglu, R. K., and Adeli, K. (2005) Intestinal assembly and secretion of highly dense/lipid-poor apolipoprotein B48-containing lipoprotein particles in the fasting state: evidence for induction by insulin resistance and exogenous fatty acids. *Metabolism*. **54**, 689–697
 91. Council, N. R., and Guide for the Care and Use of Laboratory Animals (2011) National Research Council (US) Committee for the Update of the Guide for the Care and Use of Laboratory Animals. National Academies Press, Washington. <https://doi.org/10.17226/12910>
 92. Ko, C. W., Qu, J., Liu, M., Black, D. D., and Tso, P. (2019) Use of isotope tracers to assess lipid absorption in conscious lymph fistula mice. *Curr. Protoc. Mouse Biol.* **9**, e60
 93. Millar, J. S., Cromley, D. A., McCoy, M. G., Rader, D. J., and Billheimer, J. T. (2005) Determining hepatic triglyceride production in mice: comparison of poloxamer 407 with Triton WR-1339. *J. Lipid Res.* **46**, 2023–2028
 94. Kohan, A. B., Wang, F., Lo, C-M., Liu, M., and Tso, P. (2015) ApoA-IV: current and emerging roles in intestinal lipid metabolism, glucose homeostasis, and satiety. *Am. J. Physiol. Gastrointest. Liver Physiol.* **308**, G472–G481
 95. Kohan, A. B., Wang, F., Li, X., Vandarsall, A. E., Huesman, S., Xu, M., et al. (2013) Is apolipoprotein A-IV rate limiting in the

- intestinal transport and absorption of triglyceride? *Am. J. Physiol. Gastrointest. Liver Physiol.* **304**, G1128–G1135
96. Terpstra, A. H. (1985) Isolation of serum chylomicrons prior to density gradient ultracentrifugation of other serum lipoprotein classes. *Anal. Biochem.* **150**, 221–227
97. Macpherson, A. J., and Smith, K. (2006) Mesenteric lymph nodes at the center of immune anatomy. *J. Exp. Med.* **203**, 497–500
98. MacPherson, A. J., Slack, E., Geuking, M. B., and McCoy, K. D. (2009) The mucosal firewalls against commensal intestinal microbes. *Semin. Immunopathol.* **31**, 145–149
99. Balmer, M. L., Slack, E., de Gottardi, A., Lawson, M. A., Hapfelmeier, S., Miele, L., *et al.* (2014) The liver may act as a firewall mediating mutualism between the host and its gut commensal microbiota. *Sci. Transl. Med.* **6**, 237ra66